Journal of Alloys and Compounds 503 (2010) 380–383

Contents lists available at ScienceDirect

Journal of Alloys and Compounds

journal homepage: www.elsevier.com/locate/jallcom

Crystal growth and spectroscopic properties of MoO_3 and WO_3 doped $Bi_4Ge_3O_{12}$ by optical floating zone method

Pingsheng Yu[a,b], Anhua Wu[b], Liangbi Su[b,*], Xin Guo[b], YaBin Wang[c], Hengyu Zhao[a,b], Yan Yang[b], Qiuhong Yang[a], Jun Xu[b,*]

[a] School of Materials Science and Engineering, Shanghai University, Shanghai 200072, China
[b] Key Laboratory of Transparent and Opto-Functional Inorganic Materials, Chinese Academy of Sciences, Shanghai Institute of Ceramics, Shanghai 200050, China
[c] School of Sciences, Shanghai University, Shanghai 200444, China

ARTICLE INFO

Article history:
Received 27 January 2010
Received in revised form 22 March 2010
Accepted 30 March 2010
Available online 8 April 2010

Keywords:
Optical floating zone
$Bi_4Ge_3O_{12}$
MoO_3
WO_3

ABSTRACT

MoO_3 and WO_3 doped $Bi_4Ge_3O_{12}$ (BGO) crystals were grown by the optical floating zone (OFZ) method. The structure of doped crystals was determined by XRD. The fluorescence spectra and fluorescence decay curves of these BGO crystals at room temperature were also studied. The emission intensity of BGO crystals increased with WO_3 dopant but decreased with MoO_3 dopant. A heavily WO_3 doped BGO has shown a much shorter decay time than undoped BGO at about 500 nm.

1. Introduction

The bismuth germanate–$Bi_4Ge_3O_{12}$ (BGO) single crystal is a well-known material widely used as a scintillator, and the scintillation properties of BGO have been the focus of many studies [1–4]. BGO crystal is non-hygroscopic, and has large X (or γ)-ray absorption coefficient, high effective atomic number and density (higher resistivity to radiation damages) [5–8], low afterglow, mechanical stability and an emission spectrum matching well that of semiconductor photodetectors. So, it has extensive applications in many fields ranging from high-energy and nuclear physics to medical equipment, as a detector of X-ray and γ-ray in nuclear medicine instrument, and so on. The structure of BGO consists of a regular arrangement of GeO_4 tetrahedron, and distorted BiO_6 octahedron sharing oxygen atoms of the GeO_4. The GeO_4 sublattice is considered to be stable, and most defects are therefore likely to be associated with the BiO_6 sublattice [9–12]. A directed solidification (Bridgeman), conventional Czochralski (Cz) and low-thermal-gradient Czochralski (LTG Cz) [13] techniques are known to be used for growing BGO. In this work, we used the optical floating zone (OFZ) method to grow the MoO_3 and WO_3 doped BGO crystals, and their spectra properties were investigated.

2. Experimental procedures

2.1. Optical floating zone technique

The floating zone technique using halogen lamps and ellipsoidal mirrors (often called optical floating zone, OFZ) has been employed for crystal growth of a wide range of materials, including metals, oxides and semiconductors. With a growing number of optical systems around the world this technique is gaining popularity as the method of choice for the growth of various non-conventional oxides including high temperature superconductors and new magnetic materials [14–18]. Crystals grown by the optical floating zone technique are of good quality but they are relatively small (usually not bigger than a few mm in diameter and a few cm in length), so it is usually used to grow new materials for research purposes.

2.2. Experiment

The MoO_3 and WO_3 doped BGO single crystals were grown by OFZ method in Ar atmosphere. The starting powder materials were Bi_2O_3, GeO_2, MoO_3 and WO_3 of 99.99% purity.

We prepared 5 series of BGO raw materials with different component, as presented in Table 1.

For sample No. 3, Bi_2O_3 and GeO_2 were carefully weighed with molar ratio of 2:3 to achieve the desired phase with the composition $Bi_4Ge_3O_{12}$. The chemical reaction is given by:

$$2Bi_2O_3 + 3GeO_2 \rightarrow Bi_4Ge_3O_{12}$$

The raw materials were thoroughly mixed for 24 h. For samples 1, 2, 4 and 5, we added MoO_3 or WO_3 to the mixture with a corresponding reduction of GeO_2, respectively.

The first step of rod preparation was a typical ceramics synthesis. The batch of powders were weighed according to the chemical reaction and prepared by ball mixing and then by manual or automatic grinding in the mortar. Mixture was sin-

---

* Corresponding authors. Tel.: +86 21 69987573; fax: +86 21 69987109.
E-mail addresses: su_lb@163.com (L. Su), xujun@mail.shcnc.ac.cn (J. Xu).

0925-8388/$ – see front matter © 2010 Elsevier B.V. All rights reserved.
doi:10.1016/j.jallcom.2010.03.238

Table 1
Components of BGO samples (raw materials).

No.	Bi_2O_3 (mol)	GeO_2 (mol)	MoO_3 (mol)	WO_3 (mol)
1	0.667	1–0.015	0.015	0
2	0.667	1–0.005	0.005	0
3	0.667	1	0	0
4	0.667	1–0.015	0	0.015
5	0.667	1–0.005	0	0.005

tered at an appropriate temperature for specific time (generally sintered at 300 °C for 2 h). The prepared powders were assessed by X-ray diffraction and formed as a rod (about 7 mm in diameter and 120–150 mm in length) by isopressing. The pressure had to be experimentally selected to avoid "overpressing" with the typical range of 55–65 MPa. Then the pressed rod was sintered at an optimized temperature. The as-grown crystal diameter, length and shape were governed mainly by upper rod. In this work, the type of optical floating zone furnace was FZ-T-10000-H-VI-P-SH.

3. Results and discussion

As the viscosity of melted BGO in floating zone was quite low, the growth speed should be relatively high. In our experiments, about 10 mm/h was proved to be appropriate. These crystals were grown in Ar atmosphere to keep away from O_2.

The MoO_3 concentrations in the raw materials of samples No. 1 and 2 were 1.5 mol% and 0.5 mol% relative to GeO_2, while the concentrations of Mo in the BGO crystals were checked out 3.0 mol% and 1.3 mol%, respectively, by ICP-AES (Inductively Coupled Plasma Atomic Emission Spectrometry). The WO_3 concentrations in the raw materials of samples No. 4 and 5 were 1.5 mol% and 0.5 mol% relative to GeO_2, while checked out 3.6 mol% and 0.89 mol% in the crystals, respectively. The segregation coefficient of MoO_3 and WO_3 doped crystals were all greater than 1. It could be explained by the higher viscosity of melted W:BGO or Mo:BGO than that of pure BGO, we assume that some melt of pure BGO flowed away for its relatively low viscosity, so the concentrations of W or Mo in the crystals have increased.

The MoO_3 and WO_3 doped BGO crystals, grown by OFZ method, are of good quality but they are relatively small.

View of the typical as-grown crystal is given in Fig. 1.

The XRD spectrum for 1.5 mol%WO_3 (sample 4) doped BGO crystal shows a typical structure of pure BGO (cubic symmetry with space group 43m) with a large peak centered at $2\theta = 31.8°$, shown in Fig. 2.

The light yield and the decay time of these samples of BGO crystals in visible band were measured under identical conditions, as shown in Figs. 3–7. The visible emission spectra were taken with a fluorolog-3 jobin yvon spectrophotometer.

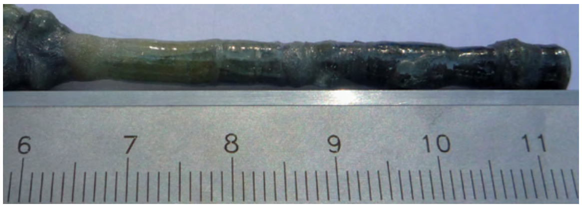

Fig. 1. Photo of 1.5 mol%MoO_3 doped BGO crystal.

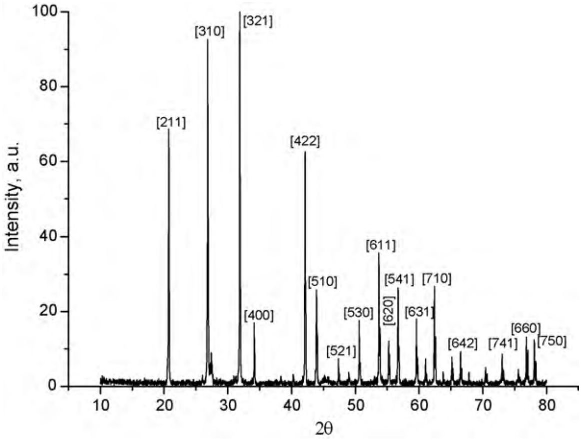

Fig. 2. X-ray diffraction pattern of 1.5 mol%WO_3 doped BGO crystal.

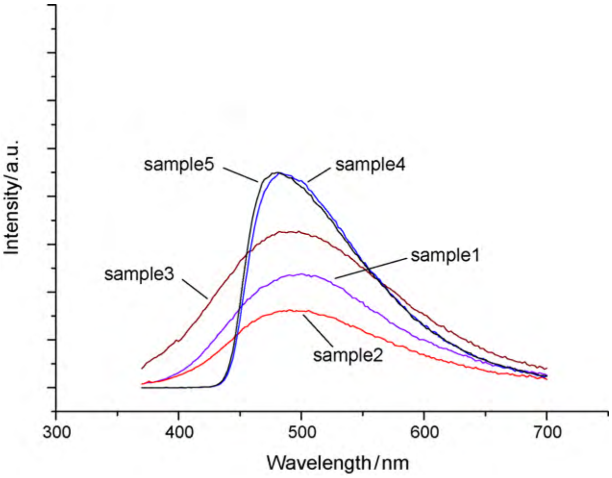

Fig. 3. Visible emission spectra (samples 1, 2, 4 and 5 under 281 nm Xenon lamp exciting, sample 3 under 304 nm Xenon lamp exciting).

Visible emission spectra are shown in Fig. 3. All samples show typical emission band peaking around 500 nm [19]. The emission intensity of Mo:BGO is weaker than that of undoped BGO, while that of W:BGO is stronger with the peak moving to shorter wavelength. Fig. 4 shows the visible luminescence and corresponding excitation spectra of 1.5 mol%MoO_3 doped BGO crystal. Fig. 5 shows the visible luminescence and corresponding excitation spectra of pure BGO crystal. The emission decay curves of sample 4 and sample 5 at about 500 nm are shown in Figs. 6 and 7. The decay curve shows that the decay time of the 1.5 mol% WO_3 doped BGO (sample 4) is 12.2 ns, which is much shorter than that of pure BGO (about 300 ns)[20]. The decay time of the 0.5 mol% WO_3 doped BGO (sample 5) is 345 ns, and those of MoO_3 doped BGO crystals are both about 330 ns. Mo^{6+} did not markedly influence the decay time of

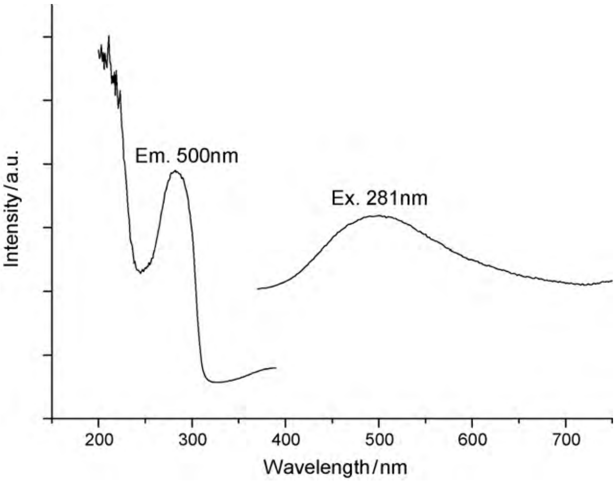

Fig. 4. Visible luminescence and corresponding excitation spectra of 1.5 mol%MoO_3 doped BGO crystal.

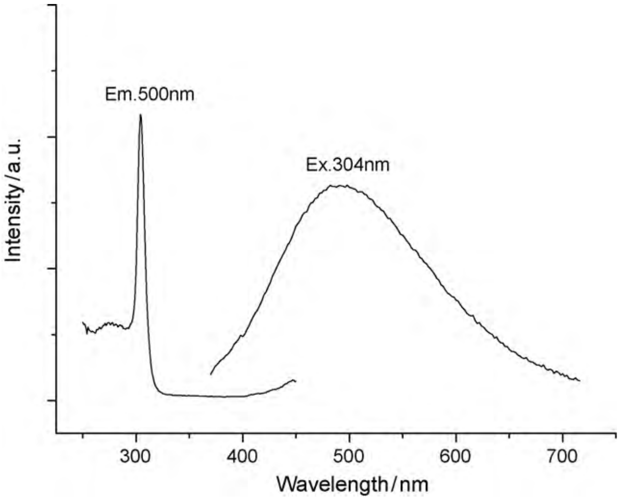

Fig. 5. Visible luminescence and corresponding excitation spectra of pure BGO crystal.

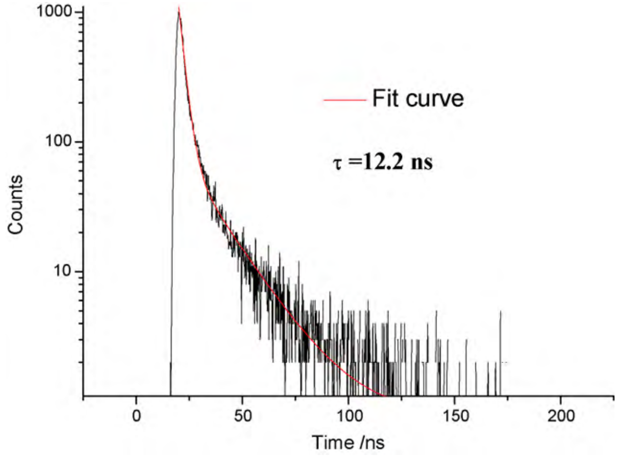

Fig. 6. The emission decay curve of sample 4 at about 500 nm.

MoO_3 doped BGO but W^{6+} did, which indicates that crystal lattice defect induced by unequal valence exchange could not be the reason for the emergence of shorter decay time of 1.5 mol% WO_3 doped BGO. It has been reported that the decay time of tungstate scintillator is 10^{-8} s order, while that of molybdate is 10^{-6} s order [21,22], which is the partial reason to explain above. There is a fact worth noting that sample 4 was checked out 3.6 mol% W in the as-grown crystal. We suppose that "WO_4" structure should be formed in BGO crystal. The group of "WO_4" is origin of the "fast blue" component of emission in $PbWO_4$, which should induce the emission peak of simple 4 shifting to shorter wavelength and the decay time becoming much shorter. However, the "quantity" of the "WO_4" is not enough to influence the structure of BGO because the XRD analysis (Fig. 2) indicates that W does not change the structure of BGO crystal, so the emission spectra of W:BGO are like that of typical pure BGO. In addition, there is an inexplicable thing, why the decay time of little WO_3 doped BGO (sample 5) is 345 ns? Perhaps only the heavily doping of WO_3 in BGO (sample 4) could change the emission mechanism.

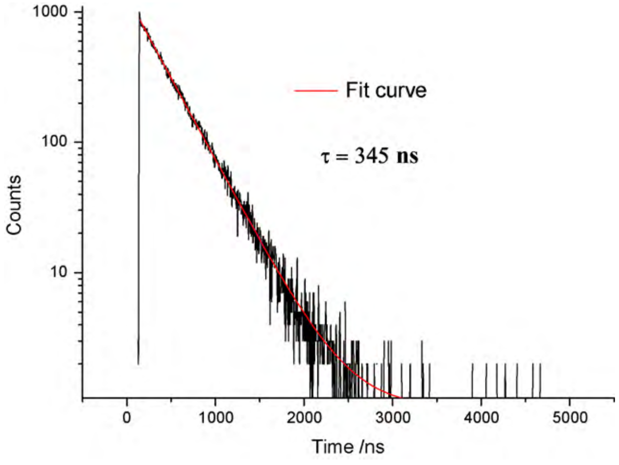

Fig. 7. The emission decay curve of sample 5 at about 500 nm.

4. Conclusions

It is the first time to prepare $Bi_4Ge_3O_{12}$ by OFZ method. The density of BGO is relatively large ($\rho = 7.13\,g/cm^3$), while the viscidity of BGO melt is quite low, which is disadvantage to use the OFZ method to grow BGO crystals. We choose the smaller power halide lamp to heat, and use faster growth speed, then grew the crystals smoothly. The grown crystals are of good quality but they are relatively small. The crystals were tested by means of XRD, and the fluorescence spectra and fluorescence decay curves of these BGO crystals at room temperature were also studied. The WO_3 doped BGO crystals have shown higher emission intensity under 281 nm Xenon lamp exciting as compared with the pure BGO at about 500 nm, while the emission intensity of MoO_3 doped BGO crystals decrease at the same wavelength. The decay time of the 1.5 mol% WO_3 doped BGO (sample 4) is much shorter than that of pure BGO. We suppose that "WO_4" structure was formed in BGO crystal. However, to explain the role of MoO_3 and WO_3 in the BGO crystals needs the further research.

Acknowledgements

This work was supported by National Natural Science Foundation of China under the No. 60778036 and 60938001, Shanghai National Natural Science Foundation under the number of 08ZR1421700, and Hundred Talents Project of the Chinese Academy of Sciences. The authors are grateful to Xiaoming Fang and Prof. Xinnian Li for their help.

References

[1] Winicjusz Drozdowski, A.J. Wojtowicz, S.M. Kaczmarek, M. Berkowski, Physica B 405 (2010) 1647.
[2] H. Farhi, S. Belkahla, K. Lebbou, C. Dujardin, Phys. Procedia 2 (2009) 819.
[3] N. Coron, E. Garcia, J. Gironnet, J. Leblanc, P. de Marcillac, M. Martinez, Y. Ortigoza, Opt. Mater. 31 (2009) 1393.
[4] J.A. Hernandez, E. Camarillo, H. Loro, H.S. Murrieta, J. Alloys Compd 323 (2001) 714.
[5] M.J. Weber, R.R. Monchamp, J. Appl. Phys. 44 (1973) 5495.
[6] O.H. Nestor, C.Y. Huang, IEEE Trans. Nucl. Sci. NS 22 (1975) 68.
[7] H. Schweppe, IEEE Trans. Son. Ultrason. SU 16 (1969) 219.
[8] M.J. Weber, J. Lumin. 100 (2002) 35.
[9] D. Bravo, F.J. Lopez, Opt. Mater. 13 (1999) 141.
[10] D. Bravo, A. Martin, A.A. Kaminskii, F.J. Lopez, Radiat. Eff. Defects Solids 135 (1995) 191.
[11] D.J. Segal, R.P. Santoro, R.E. Newnham, Z. Kristallogr. 123 (1966) 73.
[12] A.A. Kaminskii, D. Schultze, B. Hermoneit, S.E. Sarkisov, L. Li, J. Bohm, P. Reiche, R. Ehlert, A.A. Mayer, V.A. Lomonov, V.A. Balashov, Phys. Stat. Sol. A 33 (1976) 737.
[13] Ya.V. Vasiliev, R.R. Akhmetshinb, Yu.A. Borovlieva, D.N. Grigorievb, V.A. Gusevc, V.N. Shlegela, V.P. Smakhtinb, Nucl. Instrum. Methods A 379 (1996) 533.
[14] S. Kimura, K. Kitamura, A. Review, J. Am. Ceram. Soc. 75 (1992) 1140.
[15] A.M. Balbashov, S.K. Egorov, J. Cryst. Growth 52 (1981) 498.
[16] I. Shindo, J. Cryst. Growth 50 (1980) 839.
[17] B. Moest, V.G. Glebovsky, H.H. Brongersma, R.H. Bergmans, A.W. Denier van der Gon, V.N. Semenov, J. Cryst. Growth 192 (1998) 410.
[18] A. Revcolevschi, J. Jegoudez, Rev. Prog. Mater. Sci. 42 (1997) 321.

[19] R. Kibar, A. Çetin, Y. Tuncer, S. Uysal, P.D. Townsend, A. Canimoglu, T. Karali, N. Can, Phys. Procedia 2 (2009) 379.
[20] J. Gironnet, V.B. Mikhailik, H. Kraus, P. de Marcillac, N. Coron, Nucl. Instrum. Methods A 594 (2008) 358.
[21] M. Minowa, K. Itakura, S. Moriyama, W. Ootani, Nucl. Instrum. Methods A 320 (1992) 500.
[22] K. Nitsch, M. Nikl, R. Uecker, Czechoslovak J. Phys. 47 (1997) 717.